

PHYSICS OF TITANIUM ALLOYS\*-II: FERMI  
DENSITY-OF-STATES PROPERTIES, AND PHASE  
STABILITY OF Ti-Al AND Ti-Mo

E. W. Collings, J. C. Ho<sup>†</sup>, and R. I. Jaffee  
BATTELLE  
Columbus Laboratories  
Columbus, Ohio 43201

The results of magnetic and calorimetric measurements leading to evaluations of the Fermi densities-of-states,  $n(E_F)$  and Debye temperatures,  $\Theta_D$ , of Ti-Al and Ti-Mo alloys in various structural states are presented. Phase stability in these systems is correlated with the observed variations of  $n(E_F)$  and  $\Theta_D$  with electron-to-atom ratio,  $Z$ ; and the paper concludes with some general comments on the relationships between physical properties and phase stability in transition-metal binary alloys, and Ti-base alloys in particular.

\*Supported by the Air Force Materials Laboratory, WPAFB, Ohio, under Contract AF33(615)69-C-1594; and the U. S. Air Force Office of Scientific Research (AFSC) under Grant No. 71-2084.

<sup>†</sup>Present address: Department of Physics, Wichita State University, Wichita, Kansas, 67208.

## 1. INTRODUCTION

### 1.1 Specimen Materials - Experimental Techniques

In an investigation of the electronic bases of phase stability and solid-solution strengthening in Ti alloys, physical property measurements were made on specimens of Ti-Al and Ti-Mo alloys as typical examples of " $\alpha$ -stabilized" and " $\beta$ -stabilized" systems, respectively. Although a great deal of useful information was derived from measurements of a pair of electrical transport properties viz. resistivity(1), and Hall coefficient(2), the principal experimental techniques used in the study were low-temperature calorimetry augmented by magnetic susceptibility.

The low-temperature specific heat,  $C = \gamma T + \beta T^3$ , when plotted in the format  $C/T$  vs  $T^2$  yields as intercept, the electronic specific heat coefficient  $\gamma$  [leading to  $n(E_F)$ , the Fermi density-of-states] and as slope ( $\beta \propto \Theta_D^{-3}$ ) the Debye temperature  $\Theta_D$ . Also, as discussed in the companion paper (henceforth I) if the specimens become superconducting within the temperature range of the calorimeter, the specific heat measurements yield a wealth of information regarding the superconducting transition. Magnetic susceptibility,  $\chi$ , was used as adjunct to the low-temperature specific heat investigations. Since  $\chi$  contains a separable component,  $\chi_{\text{spin}}$ , which also depends on  $n(E_F)$  the magnetic susceptibility technique was used to confirm and extend the results of the calorimetric measurements. Magnetic susceptibility is a simple, rapid, and economical measurement, requiring only relatively small specimens (100 mg compared with  $\sim 30$ g for specific heat). It can be employed advantageously when a detailed study is required of the response of  $\langle n(E_F) \rangle_{\text{av}}$  to a wide range of alloy solute concentrations and heat treatments (such as quench temperatures and aging conditions). In addition the susceptibility technique can be used to investigate the  $n(E_F)$  properties of alloy phases stable only at elevated temperatures and, therefore, inaccessible to low-temperature calorimetry.

### 1.2 Experimental Program

(a) The results of magnetic susceptibility and low-temperature specific heat measurements on " $\beta$ -quenched" Ti-Mo alloys; and " $\alpha$ -quenched", and otherwise heat-treated, Ti-Al alloys were presented in the previous International Titanium Conference.(3) (b) In order to determine the  $n(E_F)$  behavior of single-phase-bcc (i.e.,  $\beta$ ) Ti-Mo alloys in the electron-to-atom-ratio (  $\bar{z}$  ) range below about 4.3, in which they are not stable at ordinary temperatures, use was made of elevated-temperature magnetic susceptibility data in the manner indicated in the companion paper (I). A comparison of the results with

those for the as-quenched alloys showed that  $\langle n(E_F) \rangle_{av}$  was relatively low in the latter due to the presence of  $\omega$ -phase precipitates.

(c) As confirmation of this conclusion, and in order to determine some of the physical properties of  $\omega$ -phase itself, magnetic and calorimetric measurements were made as a function of  $\omega$ -phase development to "metastable equilibrium"<sup>(4)</sup> through moderate-temperature (350° C) aging.

### 1.3 Data Analysis

An aim of the analytical procedure was to determine  $n(E_F)$ , a fairly fundamental quantity, and one which may be compared with the results of band structure calculations when such information is available. In suitable units<sup>(5)</sup>  $n(E_F) \cong 0.212 \gamma / (1 + 0.212 \gamma V_{app})$ , where the denominator is the electronic-specific-heat electron-phonon enhancement factor. When dealing with a family of transition-metal alloy superconductors the calorimetric data itself may contain sufficient information which, if expressible in the form of a linear  $\log (T_c/\Theta_D)$  vs  $(0.212 \gamma)^{-1}$  plot of slope  $-1/V_{app}$ , enables the electron-phonon correction to be readily applied.<sup>(6)</sup> Such was, in fact, the case for Ti-Mo alloys, including  $\alpha$ -Ti, as has already been shown<sup>(7)</sup>. Values of  $n(E_F)$  [ $\cong 0.212 \gamma / (1 + 0.212 V_{app} \gamma)$ ], calculated by applying the electron-phonon correction with  $V_{app} = 0.26$  eV-atom,

Table I. Debye Temperature,  $\Theta_D$ , And Fermi Density-of-States,  $n(E_F)$ , For Alloys in Electron-to-Atom-Ratio ( $\beta$ ) Ranges  $3.63 \leq \beta \leq 4.08$  And  $6.05 \leq \beta \leq 6.76$

Alloy*	" $\beta$ "	Phase	$\Theta_D$	$n(E_F)$	Alloy	$\beta$	Phase	$\Theta_D$	$n(E_F)$
HP-37	3.63	$[\alpha_2]$	495	0.50 <sub>1</sub>	Pure Ti	4.00	$\alpha$	420	0.60
HP-33.3	3.66	$[\alpha_2]$	506	0.48 <sub>2</sub>	TM-4.3	4.08	$\omega$	420	0.54 <sub>6</sub>
HP-30	3.70	$[\alpha_2]$	485	0.45 <sub>6</sub>					
HP-28	3.72	$[\alpha_2]$	518	0.41 <sub>6</sub>	MR-5	6.05	$\beta$	450	0.38 <sub>4</sub>
HP-25	3.75	$\alpha_2$	495	0.36 <sub>8</sub>	MR-10	6.10	$\beta$	440	0.45 <sub>0</sub>
HP-23	3.77	$\alpha_2$	485	0.30 <sub>3</sub>	MR-20	6.20	$\beta$	420	0.59 <sub>6</sub>
HP-20	3.80	$\alpha_2$	485	0.35 <sub>4</sub>	MR-25	6.25	$\beta$	405	0.62 <sub>6</sub>
HP-15	3.85	$\alpha$	442	0.64 <sub>4</sub>	MR-30	6.30	$\beta$	395	0.63 <sub>4</sub>
HP-13	3.87	$\alpha$	445	0.66 <sub>0</sub>	MR-40	6.40	$\beta$	340	0.67 <sub>1</sub>
HP-10	3.90	$\alpha$	413	0.64 <sub>0</sub>	MR-50	6.50	$\beta$	320	0.66 <sub>4</sub>
HP-5	3.95	$\alpha$	427	1.62 <sub>8</sub>	MR-58	6.58	$\sigma$	351	0.54 <sub>0</sub>
HP-3	3.97	$\alpha$	413	0.61 <sub>8</sub>					
HP-2	3.98	$\alpha$	403	0.61 <sub>5</sub>	MO-38	6.76	$\sigma$	371	0.54 <sub>2</sub>

\*HP, TM, MR, and MO-x represent Ti-Al, Ti-Mo, Mo-Re, and Mo-Os (x at.%) respectively.

to the measured  $\gamma$ 's for  $\beta$ -phase and  $(\beta+\omega)$ -Ti-Mo alloys have been presented in Table I of I. Also tabulated there are the directly-measured values of  $\Theta_D$ , together with a list of extrapolated  $\Theta_D$ 's for "unstable"(8)  $\beta$ -Ti-Mo ( $4.0 < \mathfrak{Z} < 4.3$ ), derived from a set of  $T_c/\Theta_D$  values(9). The  $\alpha$ -Ti-Al alloys on the other hand were "nonsuperconducting" (i.e.,  $T_c < 1.5$  K). But since pure  $\alpha$ -Ti was represented by a point on the above-mentioned semilog plot,  $V_{app} = 0.26$  eV-atom was also used in correcting  $\gamma$ Ti-Al for electron-phonon effects. The values of  $n(E_F)$  so obtained are listed (together with the directly-measured  $\Theta_D$ 's) in Table I of this paper.

## 2. RESULTS AND DISCUSSION

### 2.1 Physical Properties of $\alpha$ -, and $\alpha_2$ -Ti-Al and $\omega$ -, $(\beta+\omega)$ -, and $\beta$ -Ti-Mo Alloys

The experimental results, expressed in terms of the physical properties  $\gamma$ ,  $\chi$ , and  $\Theta_D$  for  $\alpha$ ,  $\alpha_2$ ,  $\omega$ ,  $(\beta+\omega)$ , and  $\beta$ -phase alloys, are summarized in Figure 1.

#### 2.1.1 $\Theta_D$ in Ti-Mo

Since as described in I, the Debye temperatures were separated out from a set of empirically-derived  $(T_c/\Theta_D)$ -values, some confirmation of the validity of the form of the resulting composition-dependence of  $\Theta_D$  was warranted.

Accordingly a comparison was made with  $\Theta_D$ (Ti-Cr), calculated by applying Anderson's method(10), to Fisher and Dever's(11) measured elastic constants. The results of this procedure are summarized in Figure 2. Taking into consideration the fact that, in the fairly massive ingots measured,  $\omega$ -phase seemed to make its appearance in Ti-Mo at a higher  $\mathfrak{Z}$  than was the case for Ti-Cr(12) Figure 2(c) shows that the deduced  $\Theta_D$ -composition-dependence for "virtual"(8)  $\beta$ -Ti-Mo was in good accord with that calculated for virtual  $\beta$ -Ti-Cr.  $\Theta_D$  is sensitive to the shear modulus  $C' = (c_{11}-c_{12})/2$  which as pointed out by Fisher and Dever(11) decreases relatively rapidly with decreasing  $\mathfrak{Z}$  upon entering the virtual- $\beta$  regime. This behavior is reflected in Figure 2(c). For Ti-Cr, martensitic transformation which has been observed within  $4.10 < \mathfrak{Z} < 4.12$ (13) seems to be related to the vanishing of  $C'$  which Figure 2(a) shows as occurring at Ti-Cr(5.03 at.%) or  $\mathfrak{Z} = 4.1$ . At the same time, Anderson's formula yields  $\Theta_D = 208$  K; a value which tends to confirm the independently deduced behavior of  $\Theta_D$  (Ti-Mo) which drops to 207 K at 5 at.% Mo, just prior to martensitic transformation at 4-1/2 at.% Mo(14). Whereas the martensitic transformation is undoubtedly associated with  $C' = 0$ (4,11) (i.e., "softening"(15)), de Fontaine *et al*(4) have shown that the  $\beta \rightarrow \omega$  transformation can be achieved formally by altering

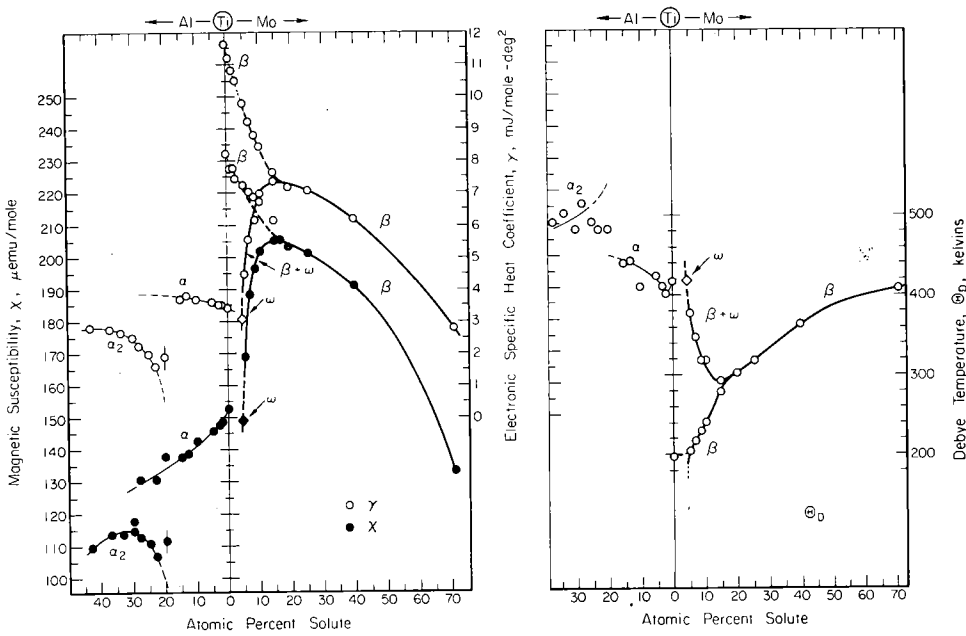


Figure 1. Composition-dependences of magnetic susceptibility ( $\chi$ ), low-temperature-specific-heat coefficient ( $\gamma$ ), and Debye temperature ( $\Theta_D$ ), for Ti-Al and Ti-Mo alloys in various structural states viz.:  $\alpha_2$ ,  $\alpha$  (Ti-Al); and  $\alpha$ ,  $\omega$ ,  $\omega + \beta$ , and  $\beta$  (Ti-Mo).

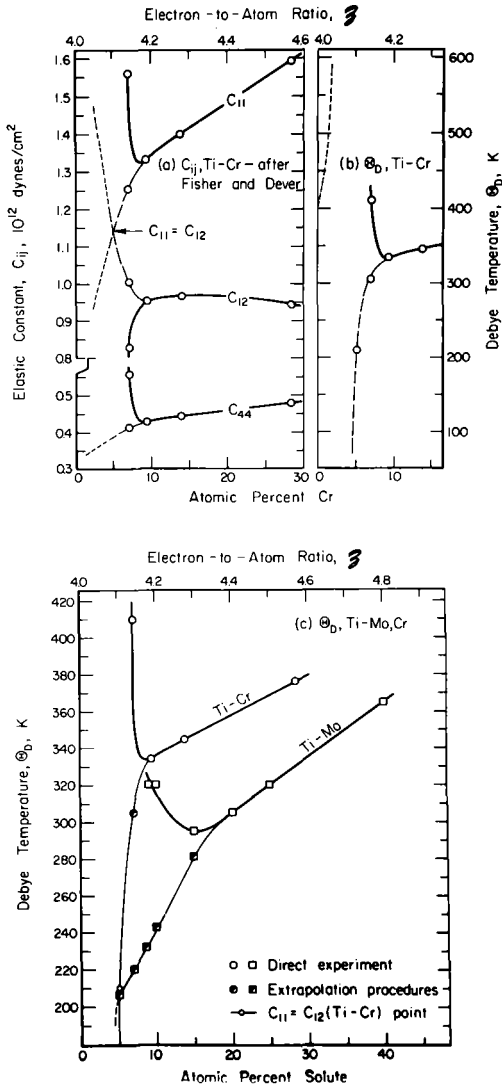


Figure 2. (a) Elastic constants  $c_{11}$ ,  $c_{12}$  and  $c_{44}$  of Ti-Cr - after Fisher and Dever(11,16). (b)  $\Theta_D$  for Ti-Cr calculated from the data of the previous figure, using Anderson's(10) method. (c) Comparison of the temperature-dependence of  $\Theta_D$  for Ti-Cr and Ti-Mo. At the observed room-temperature threshold of martensitic transformation for Ti-Mo (viz. 4-1/2 at.%), and when  $c_{11} = c_{12}$  for Ti-Cr, we find  $\Theta_D^{Ti-Mo} \approx \Theta_D^{Ti-Cr} = 208$  K.

the atomic force constants at constant  $c_{ij}$ . In practice, however, it seems that it is in fact a "weakening"<sup>(16)</sup> of  $C'$  (as the softening-point,  $C' = 0$ , is approached) which leads to displacement fluctuations<sup>(4)</sup> of sufficient amplitude to excite the  $\beta \rightarrow \omega$  diffusionless transformation.

## 2.2 Physical Properties of $\omega$ -Phase in Ti-Mo

In an aging study, Ti-Mo (10 at.%) (TM-10) was annealed at 350°C for 880 hours, by which time it was assumed that a condition approximating quasi-equilibrium had been attained as represented by the metastable phase diagram of Reference (4). The evaluation of  $f_\omega$ , the mole-fraction of  $\omega$ -phase present in the aged TM-10 has been discussed in I. If  $\phi$  is then taken to represent the physical properties  $\chi$ ,  $\gamma$ , and  $\Theta_D$  in turn, the conservation equation:

$$\langle \phi \rangle_{av} = f_\omega \phi_\omega + (1-f_\omega) \phi_\beta, \quad (1)$$

together with the previously estimated values of  $\phi_\beta$ , may be used to determine  $\chi_\omega$ ,  $\gamma_\omega$ , and  $\Theta_{D,\omega}$  for  $\omega$ -TM-4.3. The values so obtained, plotted as special points in Figure 1, are seen to be in excellent agreement with the directly measured quantities for  $(\beta+\omega)$ -Ti-Mo. These results serve to confirm that the decreases in  $\chi$  and  $\gamma$  with decreasing  $\mathcal{Z}$  ( $\lesssim 4.3$ ) as well as the corresponding stiffening of  $\Theta_D$  are, in fact, due to the continuously increasing influence of  $\omega$ -phase precipitation. The  $n(E_F)$  for  $\omega$ -TM-4.3, derived from  $\gamma_\omega$  using  $V_{app} = 0.26$  eV-atom as before, is listed in Table 1.

## 2.3 $n(E_F)$ and $\Theta_D$ in Ti-Al and Ti-Mo

The variations of  $n(E_F)$  and  $\Theta_D$  with  $\mathcal{Z}$ , derived as a result of the magnetic and calorimetric experiments on the  $\alpha$  and  $\alpha_2$  phases of Ti-Al, and the  $\alpha$ ,  $\omega$ ,  $\beta+\omega$ , and  $\beta$  phases of Ti-Mo are shown in Figure 3. In this Figure,  $\mathcal{Z}$  is not intended to have a real physical meaning but is to be interpreted as an arbitrary horizontal scale, based on the average number of atomic s, p and d electrons in the case of Ti-Al, and s+d electrons in the case of Ti-Mo. Particularly noticeable are (a): that the more stable (at say, room temperature) of a pair of allotropes, possesses the lower  $n(E_F)$  together with the higher  $\Theta_D$ --tightly-bound  $\alpha_2$ -Ti-Al compared to  $\alpha$ -Ti-Al is a very good example of this--and (b): that discontinuities or turning points in the  $\mathcal{Z}$ -dependence of  $n(E_F)$  [or  $\Theta_D$ , which scales inversely with it] occur at the limits of the various regimes of structural stability.

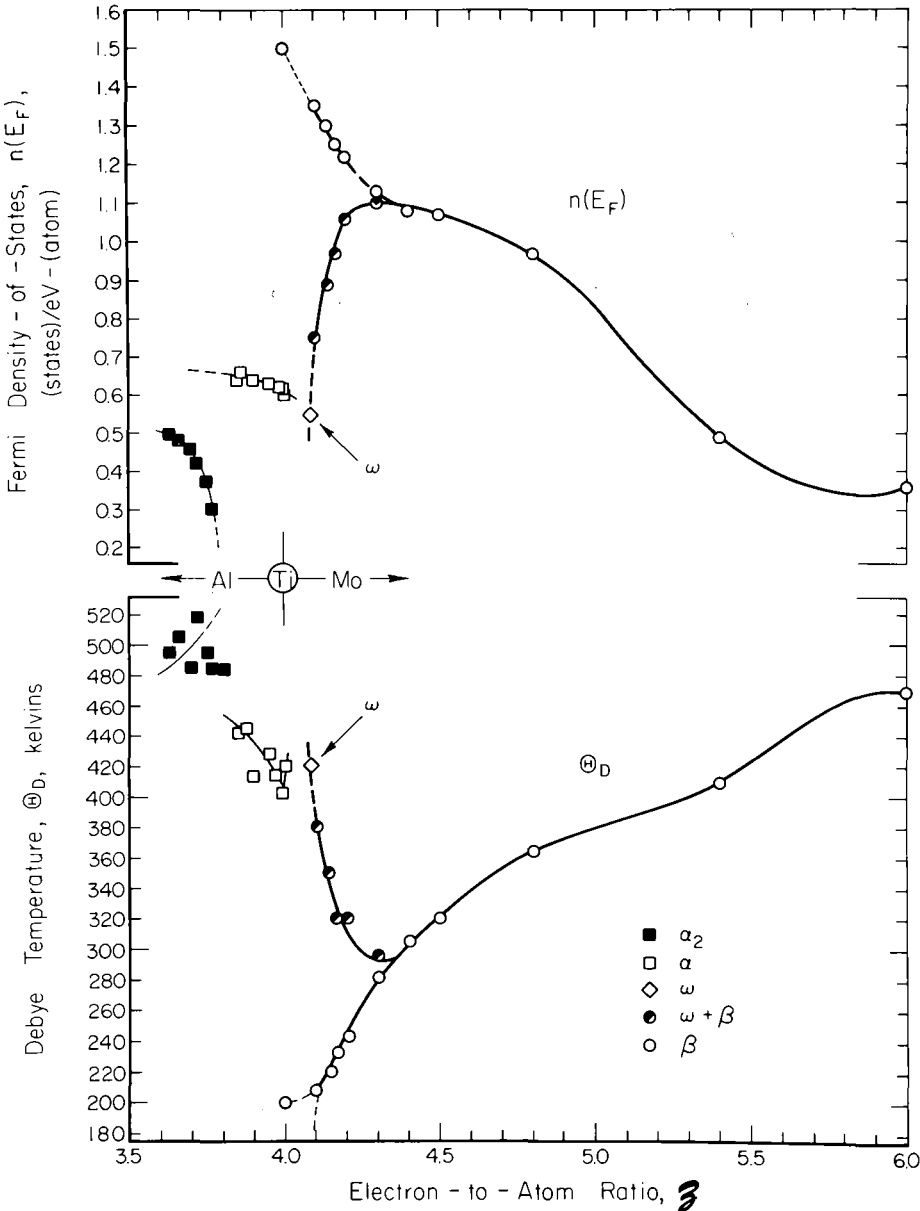


Figure 3. Empirically-derived Fermi density-of-states,  $n(E_F)$ , and Debye temperature,  $\Theta_D$ , as functions of electron-to-atom ratio,  $z$ , in Ti-base alloys.



### 2.4 Phase Stability in Titanium Alloys

Figure 4 presents an experimentally-determined  $n(E_F)$  curve for some binary transition-metal alloys within  $4 \leq \beta \leq 7$ . The  $4 \leq \beta \leq 6$  regime was covered by Ti-Mo, as described above. In order to extend the range to  $\beta = 7$ , use was made of the calorimetrically determined data for Mo-Re, and Mo-Os from the work of Morin and Maita(17) and Bucher *et al.*(18). In applying an electron-phonon correction in this range Morin and Maita's(17)  $V_{app} = 0.426$  was employed. The experimentally-derived curve may be compared with a "calculated"  $n(E_F)$ -curve based on computed(19) values of  $n(E_F)$  for *bcc* Ti, V, Cr, Mn, and Fe, and for the alloy system Ti-Mo(20). Also included for comparison as an inset, are reproductions of Waber's(20) calculated  $n(E)$  profiles for the *bcc* 3d and 4d elements Cr and Mo. Such curves for *all* *bcc* 3d transition elements as well as some *bcc* 4d transition elements are characterized by a pair of dominant peaks(21). At this stage it is appropriate to point out that, even within the context of rigid-band-type behavior [as discussed in (19)], the twin main peaks of the  $N(E)$  curves of pure *bcc* metals (see inset) are not to be confused with those apparent in the calorimetrically-derived  $n(E_F)$  loci. The latter occur "closer in" and are induced by structural transformations of the  $\beta$ -phase, which take place both for  $\beta \lesssim 4.3$  and  $\beta \gtrsim 6.7$ . Thus, the experimentally-determined maxima (e.g. that for  $\beta \sim 4.3$ ) vanish when  $n(E_F)$  is extrapolated semi-empirically into the unstable  $\beta$  regime.

De Fontaine(22) in studying the lattice dynamics of the *bcc* structure has computed with remarkable success the instability conditions leading to spontaneous ("athermal")  $\omega$ -phase formation. Presumably the upper- $\beta$  limit of *bcc* stability could also be treated in terms of atomic force constants. The ions of course interest *via* the electrons(23), but so far a rigorous electronic interpretation of transition-metal-alloy phase stability, using modern theories of metals, has not yet appeared. Figures 3 and 4, however, contain some empirical results which could perhaps serve as a starting point *viz.*:

(a) For a given  $\beta$  the more stable ( $\lesssim$  room temperature) of a pair of allotropes is associated with the lower  $n(E_F)$ . Thus, for three specific single-phase situations (Figure 3):

$$n(E_F)_{\alpha_2\text{-Ti}_3\text{Al}} < n(E_F)_{\alpha\text{-Ti}_3\text{Al}} \quad (T \lesssim 830^\circ \text{ C})$$

$$n(E_F)_{\alpha\text{-Ti}} < n(E_F)_{\beta\text{-Ti}} \quad (T \lesssim 883^\circ \text{ C})$$

$$n(E_F)_{\omega\text{-TM-4.3}} < n(E_F)_{\beta\text{-TM-4.3}} \quad (T \lesssim 500^\circ \text{ C})$$

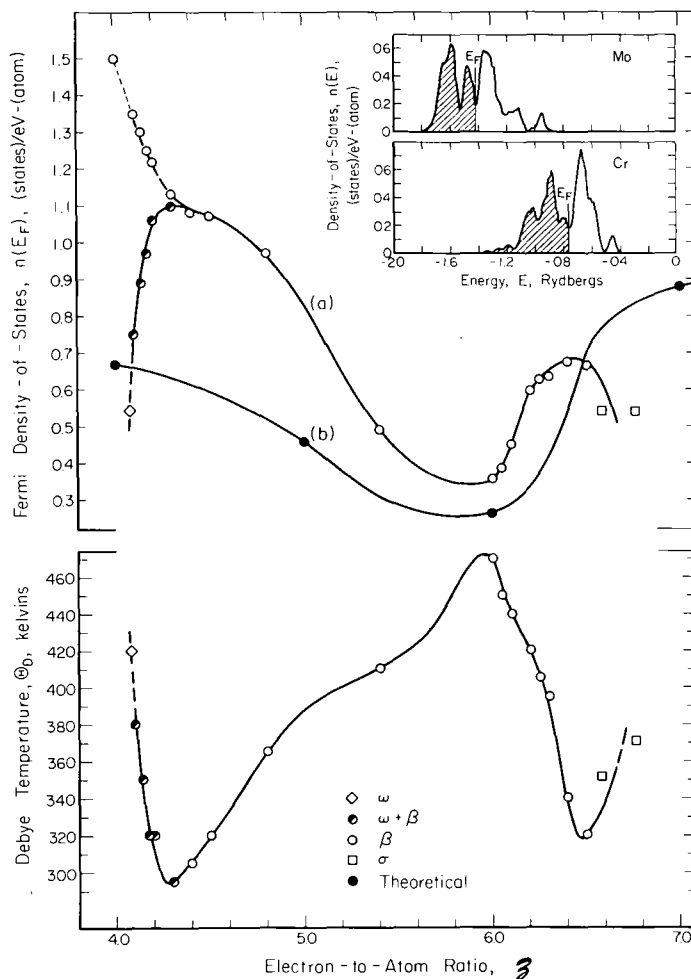


Figure 4.  $Z$ -dependence of  $n(E_F)$  for transition-metal-binary (i.e.  $T_1$ - $T_2$ ) alloys: (a) Empirically-derived curve for Ti-Mo-Re, based on the present data and those of References (17) and (18); (b) "calculated"  $n(E_F)$  for bcc  $T_1$ - $T_2$  alloys based on published data points (19) for bcc Ti, V, Cr, Mn and Fe. For comparison, the  $Z$ -dependence of  $\Theta_D$  for Ti-Mo-Re is also shown. The remarkable inverse scaling exhibited by the  $n(E_F)$  and  $\Theta_D$  curves owes its origin to phase stability-considerations.

Inset are calculated  $n(E)$  curves for bcc Ti and Mo from the work of Waber and colleagues (20).  $n(E_F)$  is at a local minimum in  $n(E)$  for both bcc Ti and Mo; however, the latter shows an extra peak, which seems to be reflected in the calculated  $n(E_F)$  for Ti-Mo (20) but not in the experimentally derived curve presented here.

(b) As  $\beta$  is varied, maximal bcc stability is achieved with a half-filled d-band. The decrease in stability as  $\beta$  either increases or decreases from this position is reflected in a decreasing  $\Theta_D$ . This, in turn, is the result of a weakening in  $C' = (c_{11} - c_{12})/2$  which has been shown to occur in each case (24, 11, respectively), and which precedes structural transformation to  $\sigma$ -phase on one hand, and  $\omega$ -phase on the other.

For Ti-base alloys, therefore, since the only way to increase the occupancy of the d-band is to add conduction electrons, transition elements tend to be  $\beta$ -stabilizers. On the other hand non-transition metals such as Al, Ga, and Sn reduce the occupancy of the Ti d-band, not only because they possess fewer conduction electrons but through the formation of bound states. These are, of course,  $\alpha$ -stabilizers.

### References

1. J. C. Ho and E. W. Collings, "Anomalous Electrical Resistivity in Titanium Molybdenum Alloys", Acta. Met., ---submitted for publication.
2. J. C. Ho, P. C. Gehlen, and E. W. Collings, Solid State Comm. 7 511 (1969).
3. E. W. Collings and J. C. Ho, "The Science Technology and Application of Titanium", Proceedings of an International Conference, London, May, 1968; ed. R. I. Jaffee and N. E. Promisel, Pergamon Press Ltd. (1970) p. 331.
4. D. de Fontaine, N. E. Paton, and J. C. William, Acta Met., 19 1153 (1971).
5. The units of  $n(E_F)$  are taken to be states/eV-atom considering a single spin direction (i.e., half the total density-of-states); and those of  $\gamma$  are mJ/mole-deg<sup>2</sup> K.
6. E. W. Collings and J. C. Ho, phys. stat. sol. (b) 43 K123 (1971).
7. See Figure 3 of Paper I.
8. Referring to single-phase-bcc ( $\beta$ ) Ti-Mo we have designated several electron-to-atom-ratio ( $\beta$ ) regimes as follows:  
 $4.0 \leq \beta \leq 4.3$  - "unstable"; a regime which includes  
 (i)  $4.0 \leq \beta \leq 4.05$  - "absolutely unstable", and  
 (ii)  $4.05 \leq \beta \leq 4.3$  - "virtual".
9. E. W. Collings, J. C. Ho, and R. I. Jaffee "Superconducting Transition Temperature, Lattice Instability, and Electron-to-

- Atom Ratio in Transition Metal Binary Solid Solutions", Phys. Rev.--to be published.
10. O. S. Anderson, J. Phys. Chem, Solids, 24 909 (1963).
  11. E. S. Fisher and D. Dever, Acta Met., 18 265 (1970).
  12. The microstructures of quenched Ti-Cr and Ti-Mo are reviewed in Appendix 3 of Reference (9).
  13. P. Duwez and J. L. Taylor, Trans. ASM, 44 495 (1952).
  14. E. W. Collings and J. C. Ho, Phys. Rev. B, 1 4289 (1970).
  15. Whereas a significant decrease in  $C'$  might reasonably be referred to as "softening", Fisher and Dever<sup>(16)</sup> would refer to this as "weakening"; while de Fontaine et al.<sup>(4)</sup> reserve the term "softening" for  $C' \rightarrow 0$ .
  16. E. S. Fisher and D. Dever, "The Science Technology and Application of Titanium", Proceedings of an International Conference, London, May, 1968; ed. R. I. Jaffee and N. E. Promisel, Pergamon Press Ltd. (1970) p. 373.
  17. F. J. Morin and J. P. Maita, Phys. Rev., 129 1115 (1963).
  18. E. Bucher, F. Heiniger, and J. Muller, Phys. kondens. Materie, 2 210 (1964).
  19. E. C. Snow and J. T. Waber, Acta Met., 17 623 (1969).
  20. J. T. Waber, in discussion to G. Broden et al., Proceedings of the 3rd Materials Research Symposium, "Electronic Density of States", Nat. Bur. Stand. (U.S.), Spec. Pub. 323, December, 1971, p. 217 (pp. 221-223).
  21. The  $n(E)$  profiles for Nb and Mo possess less-pronounced centrally-situated peaks; a property which seems to show up in the calculated  $n(E_F)$  curve for Ti-Mo alloys, but which is not shared by the experimentally observed  $n(E_F)$  for Ti-Mo.
  22. D. de Fontaine, Acta Met., 18 275 (1970).
  23. M. H. Cohen in "Alloying Behavior and Effects in Concentrated Solid Solutions", T. B. Massalski (ed.) Gordon and Breach (1965) pp. 1-23; A. Blandin. loc. cit. pp. 50-84; W. A. Harrison, "Pseudopotentials in the Theory of Metals", W. A. Benjamin, Inc. (1966).
  24. D. L. Davidson and F. R. Brotzen, J. App. Phys., 39 5768 (1968)